Chemistry & Biology
Article

Tandem Enzymatic Oxygenations in Biosynthesis of Epoxyquinone Pharmacophore of Manumycin-type Metabolites

Zhe Rui,[1] Moriah Sandy,[1] Brian Jung,[1] and Wenjun Zhang[1,*]
[1]Department of Chemical and Biomolecular Engineering and Energy Biosciences Institute, University of California, Berkeley, CA 94720, USA
*Correspondence: wjzhang@berkeley.edu
http://dx.doi.org/10.1016/j.chembiol.2013.05.006

SUMMARY

Many natural products contain epoxyquinone pharmacophore with unknown biosynthetic mechanisms. Recent genetic analysis of the asukamycin biosynthetic gene cluster proposed enzyme candidates related to epoxyquinone formation for manumycin-type metabolites. Our biochemical studies reveal that 3-amino-4-hydroxyl benzoic acid (3,4-AHBA) precursor is activated and loaded on aryl carrier protein (AsuC12) by ATP-dependent adenylase (AsuA2). AsuE1 and AsuE3, both single-component flavin-dependent monooxygenases, catalyze the exquisite regio- and enantiospecific postpolyketide synthase (PKS) assembly oxygenations. AsuE1 installs a hydroxyl group on the 3,4-AHB ring to form a 4-hydroxyquinone moiety, which is epoxidized by AsuE3 to yield the epoxyquinone functionality. Despite being a single-component monooxygenase, AsuE1 activity is elicited by AsuE2, a pathway-specific flavin reductase. We further demonstrate that the epoxyquinone moiety is critical for anti-MRSA activity by analyzing the bioactivity of various manumycin-type metabolites produced through mutasynthesis.

INTRODUCTION

The epoxyquinone family of natural products is widely distributed in nature and has been attracting much attention because of its unique structures and promising biologic activities (Miyashita and Imanishi, 2005). Examples of family members include epoxyquinol A and B (anti-angiogenic and antitumor; Kamiyama et al., 2008), preussomerins (Ras farnesyl transferase inhibitor; Singh et al., 1994), panepophenanthrin (ubiquitin-activating enzyme inhibitor; Sekizawa et al., 2002), EI-1941-1 and EI-1941-2 (interleukin-1β converting enzyme inhibitors; Koizumi et al., 2003), aranorosin (anti-apoptotic Bcl-2 inhibitor; Nakashima et al., 2008), and integrasone (HIV-1 integrase inhibitor; Herath et al., 2004; Figure S1 available online). Despite extensive efforts on the regio- and enantio-synthesis of epoxyquinone natural products, little is known regarding the biogenesis of the epoxyquinone moiety, the warhead crucial for various biologic functions exhibited by epoxyquinone metabolites.

The manumycins are a unique group of epoxyquinone natural products. Since their discovery in 1963, more than 30 manumycin-related natural products have been reported (Sattler et al., 1998). They share a common structural skeleton with a 2-amino-4-hydroxyl-5,6-epoxycyclohex-2-enone (mC_7N) core and a variety of acyl side chains on the amino nitrogen (upper side chain) and at the C4 position (lower side chain). The lower chain is further terminated by a 2-amino-3-hydroxycyclopent-2-enone (C_5N) moiety to give the manumycin-type framework (Figure 1). In addition to antibacterial, anticoccidial, and antifungal activities (Sattler et al., 1998), manumycin compounds displayed strong inhibitory activities against farnesyltransferase (Hara et al., 1993; Sugita et al., 2007), interleukin-1β converting enzyme (Tanaka et al., 1996), IkappaB kinase (Bernier et al., 2006), and acetylcholinesterase (Zheng et al., 2007), and thus are drug candidates to treat cancer, atherosclerosis, inflammation, and Alzheimer disease. We have begun to focus on the biosynthesis of asukamycins, a group of manumycin-type metabolites produced by *Streptomyces nodosus* subsp. *asukaensis* (Figure 1; Omura et al., 1976). The biosynthetic gene cluster of asukamycin was recently identified and studied using the blocked mutants of asukamycin producers (Rui et al., 2010). Although tentative gene functions were assigned based on the in vivo mutagenesis results, the enzymology of the distinct structural features embedded in asukamycins, particularly the enzymatic mechanism underlying the formation of epoxyquinone moiety (mC_7N), remained unresolved. Herein, we report the characterization of enzymes required for the biosynthesis of epoxyquinone moiety in asukamycins.

Feeding experiments indicated that mC_7N arose from 3-amino-4-hydroxyl benzoic acid (3,4-AHBA), the same biosynthetic precursor for grixazone produced by *S. griseus* (Suzuki et al., 2006). 3,4-AHBA was previously demonstrated as a condensation product of two primary metabolites, L-aspartate-4-semialdehyde (ASA) and dihydroxyacetone phosphate (DHAP), by the catalytic functions of GriI and GriH in *S. griseus* (Suzuki et al., 2006). Enzymes highly homologous to GriI and GriH, AsuA1 and AsuA3, respectively, were encoded in the *asu* gene cluster. The subsequent gene disruptions and chemical complementations with 3,4-AHBA strongly indicated that 3,4-AHBA was an en route biosynthetic intermediate to the mC_7N moiety (Rui et al., 2010). We propose that 3,4-AHBA is first activated by adenylation, presumably catalyzed by an ATP-dependent adenylase homolog AsuA2, followed by transferring of 3,4-AHBA moiety to an acyl carrier protein (ACP) for the downstream polyketide chain extensions to form the lower chain. Two

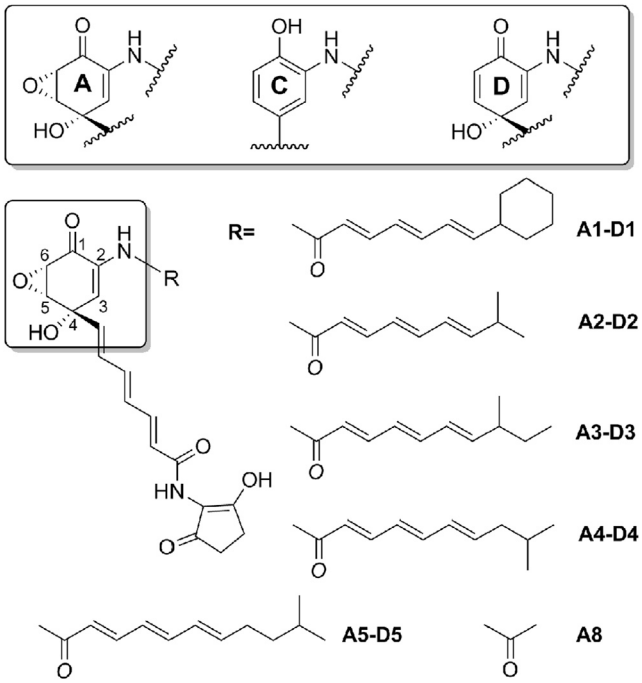

Figure 1. Chemical Structures of Manumycin-Type Compounds
Asukamycin is **A1**; protoasukamycin is **C1**; 4-hydroxyprotoasukamcyin is **D1**. See also Figure S1.

typical ACP coding genes, *asuC11* and *asuC12*, were identified in the *asu* gene cluster, yet the specificity of them has not been determined. The key reactions to convert 3,4-AHBA moiety to mC_7N, which include the de-aromatization and oxidation reactions, are proposed to take place on the biosynthetic intermediate protoasukamycin (**C1**; Figure 1) after the installation of the upper and lower chains on 3,4-AHBA. Mutant analysis further suggested that at least three oxygenases (AsuE1, AsuE2, and AsuE3) encoded in the *asu* gene cluster were related to the formation of mC_7N via insertion of hydroxyl and epoxide oxygens at the C4 and C5–C6 positions (Rui et al., 2010). With both in vitro and in vivo analysis, we provide experimental validation and probe the flexibility of the mC_7N biosynthetic pathway, including a cascade of reactions for the priming and postassembly modifications of 3,4-AHBA, to yield the epoxyquinone pharmacophore.

RESULTS AND DISCUSSION

Priming of 3,4-AHBA Starter Unit

Previous studies suggested that 3,4-AHBA is not only the precursor of epoxyquinone core, but also serves as a starter unit for the lower polyketide chain assembly of manumycin metabolites (Hu et al., 1997). We propose that 3,4-AHBA is activated by adenylation catalyzed by AsuA2 and then tethered to a specific ACP for the PKS extension possibly without the formation of 3,4-AHB-CoA thioester intermediate (Ferreras et al., 2008; Pfennig et al., 1999; Sandy et al., 2012). The ability of AsuA2 to reversibly adenylate various benzoic acid derivatives was tested using the classical ATP-[^{32}P]PP$_i$ exchange assay. AsuA2 demonstrated the activation of 3,4-AHBA, with the kinetic parameters (K_m = 21.20 μM, k_{cat} = 5.52 min^{-1}) comparable to those of typical adenylases in secondary metabolite biosynthetic pathways (Figures 2A and 2B; Sandy et al., 2012). In addition to 3,4-AHBA, various tested aryl acids were also strongly activated by AsuA2, including 4-aminobenzoic acid (4-ABA), 3,4-ACBA, 4-hydroxybenzoic acid (4-HBA), and 3-aminobenzoic acid (3-ABA) (Figure 2A). Further analysis of the activation pattern suggested that AsuA2 tolerated functional group substitutions at the meta- and para- positions rather than the ortho- position (Figure S3). Aryl-CoA products were not detected upon addition of CoA to the enzymatic reactions of AsuA2, confirming that AsuA2 functioned as an adenylation enzyme without forming a CoA thioester intermediate.

To identify the cognate loading partner of AsuA2, two ACP candidates, AsuC11 and AsuC12, were supplemented to the AsuA2 assay, respectively, and the ACPs were monitored for mass changes with liquid chromatography-mass spectrometry (LC-MS; Figures 2C and S4). An anticipated increase of 135 Da, corresponding to the formation of 3,4-AHB-*S*-ACP from holo-ACP, was observed in the reaction of AsuC12 but not of AsuC11, demonstrating that AsuC12 served as the specific ACP for 3,4-AHBA loading (Figure 2D). Other aryl acids could also be efficiently loaded onto holo-AsuC12 after activation (Figure S4), suggesting that the loading ACP (AsuC12) was promiscuous toward aryl substrates.

AsuE1 Is a Flavin-Dependent Protoasukamycin Hydroxylase

AsuE1 exhibits moderate sequence similarity to para-hydroxybenzoate hydroxylase (PHBH; identity/similarity = 22%/38%; Cole et al., 2005; Entsch et al., 2005), which catalyzes hydroxylation reactions of aromatic substrates utilizing FAD as a cofactor, NADPH as a reducing agent, and molecular oxygen to provide the oxygen atom of the incorporated hydroxyl group. The Δ*asuE1* mutant of *S. nodosus* accumulated protoasukamycin (**C1**), suggesting the substrate of AsuE1 to be **C1** (Rui et al., 2010). AsuE1 was purified from *Escherichia coli* as a colorless protein without a detectable amount of bound flavin. The incubation of AsuE1 with NADPH, FAD, and **C1** led to the formation of a compound detected with LC-MS, with the retention time and mass (m/z = 531.2491 [M + H]$^+$, ppm = 0.2) matching those of the authentic 4-hydroxyprotoasukamycin (**D1**). Control experiments showed that the formation of product depended on the presence of nicotinamide reducing agent, flavin cofactor, and the enzyme. AsuE1 displayed no significant preference toward flavin cofactors, because FAD, FMN, and riboflavin could be utilized efficiently in the catalysis (Figure 3A). AsuE1 thus belongs to the family of single-component monooxygenases: a single enzyme catalyzes both the reduction of flavin by NADPH, and the hydroxylation using molecular oxygen and reduced flavin cofactor (van Berkel et al., 2006). This is distinct from the two-component monooxygenase system which requires a separate flavin reductase component to provide the reduced flavin for the monooxgenase enzyme (Ballou et al., 2005). This finding is unanticipated due to the presence of AsuE2, a flavin reductase homolog encoded in the *asu* gene cluster, and that the disruption of *asuE2* significantly decreased the yield of asukamycin and resulted in the accumulation of **C1**.

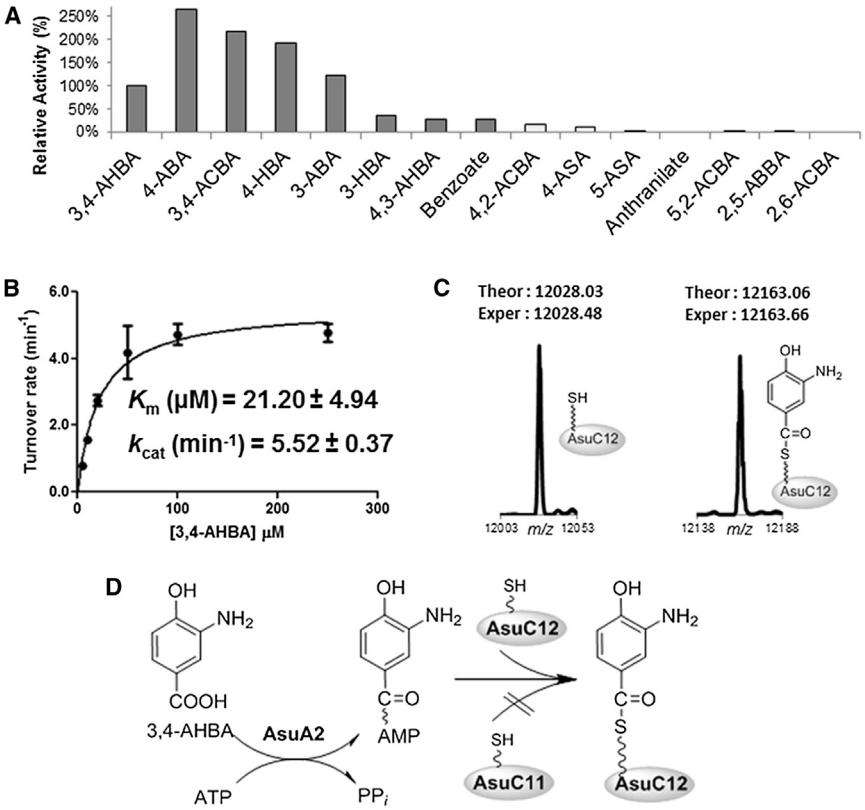

Figure 2. Characterization of AsuA2, AsuC11, and AsuC12

(A) AsuA2 activity toward various aromatic substrates in ATP-[^{32}P]PP$_i$ exchange assays. A relative activity of 100% for 3,4-AHBA-dependent exchange corresponds to 82k CPM. All chemical structures are shown in Figure S3.

(B) Determination of AsuA2 kinetic parameters by ATP-[^{32}P]PP$_i$ exchange assays. Error bars represent SDs from at least three independently performed experiments.

(C) Detection of holo-AsuC12 without AsuA2 and 3,4-AHB-*S*-AsuC12 in the AsuA2 reaction by HRMS with deconvolution.

(D) Schematic of 3,4-AHBA activation and loading. See also Figures S3 and S4.

The kinetic parameters of AsuE1 toward **C1** were determined by monitoring **D1** formation using LC-MS. The enzyme demonstrated good binding affinity toward **C1** (K_m = 21.31 μM), albeit with relatively slow turnover rate (k_{cat} = 0.183 min^{-1}) for secondary metabolism (Figure 3B). AsuE1 also converted the protoasukamycin derivatives (**C3**–**C5**) into the corresponding 4-hydroxyprotoasukamycin derivatives (**D3**–**D5**). However, AsuE1 demonstrated only trace activities to install a hydroxyl group on compounds such as 2-amino-4-methyl-phenol and ferulic acid (Figure S5) and no activity on 3,4-AHB-*S*-ACP. These results indicated the stringent substrate requirement of AsuE1 toward a triene lower chain, which is conserved in most manumycin-type metabolites.

The specificity of AsuE1 toward NAD(P)H was probed using continuous colorimetric assays. AsuE1 displayed preference toward NADH over NADPH, with k_{cat}/K_m for NADH (9.0 s^{-1}mM^{-1}) 50-fold higher than that for NADPH (0.18 s^{-1}mM^{-1}; Figure 3B). Notably, the consumption rates of nicotinamide substrates were independent of the concentration of **C1** (Figure S6), different from the catalytic mechanism of PHBH where substrate PHB must bind before initiation of reduction of the flavin (Cole et al., 2005; Entsch et al., 2005). Without aromatic substrates, the reduced flavin would react with oxygen and eliminate H_2O_2, a destructive oxidant that can be damaging to the cell. This futile cycle also wastefully consumes nicotinamide reducing agents. Due to the low overall catalytic efficiency of AsuE1, we next performed the detailed biochemical characterization of the flavin reductase homolog AsuE2 and probed the possible interplays between AsuE1 and E2 in the hydroxylation of protoasukamycin.

AsuE2 Is a Flavin-Reductase Enhancing Activity of AsuE1

AsuE2 shows high sequence similarity to flavin reductases such as HapC (identity/similarity = 33%/52%; Kim et al., 2008) and TftC (identity/similarity = 29%/41%; Webb et al., 2010) involved in the hydroxylation of 4-hydroxyphenylacetate and 2,4,5-trichlorophenol, respectively. Sequence alignment of flavin reductases revealed that AsuE2 possesses the highly conservative Tyr-178 and Val-39 to accommodate the dimethyl benzene moiety of the flavin (Webb et al., 2010) and His-151 and Ser-60 to stabilize NAD(P)H (Kim et al., 2008). Moreover, Δ*asuE2* mutant accumulated a significant amount of **C1** (Rui et al., 2010), suggesting that AsuE2 might assist the catalysis of AsuE1 by providing a reduced form of flavin in *S. nodosus*. AsuE2 contained a trace amount of FMN at a molar ratio of ~1:2,000 (FMN:AsuE2) upon purification from *E. coli* (Figure S7). The activity of AsuE2 as a flavin reductase was confirmed by colorimetric assays monitoring the consumption of NAD(P)H. With a FMN concentration of 10 μM, the enzyme showed a K_m of 171.2 μM for NADH with an apparent k_{cat} of 2.34 s^{-1}, and a K_m of 1,689 μM for NADPH with an apparent k_{cat} of 5.31 s^{-1}, indicating the preferential utilization of NADH by AsuE2 (Figure 4A).

In vitro AsuE1 assays were then performed by replacing the exogenous flavin with 1 μM of AsuE2. The time-dependent conversion of **C1** to **D1** was observed in the AsuE1/E2 assay without the addition of free flavin (Figure 4B). To probe the necessity of AsuE2, a control experiment was further conducted with 0.5 nM of exogenous FMN, the amount equivalent to the bound FMN in 1 μM of AsuE2. No **D1** was detected in the AsuE1 assay with 0.5 nM of free FMN, indicating that the observed hydroxylation activity in AsuE1/E2 reaction was due to the concerted functions of both enzymes. It is notable that there was no protein-protein interaction between AsuE1 and E2 in pull-down assays, suggesting a possible transient interaction between the two enzymes instead of forming a stable complex.

Our biochemical analysis of AsuE1 and E2 demonstrated that although the activity of AsuE1 was not affected by the AsuE2 in the presence of abundant flavin, AsuE2 elicited the activity of

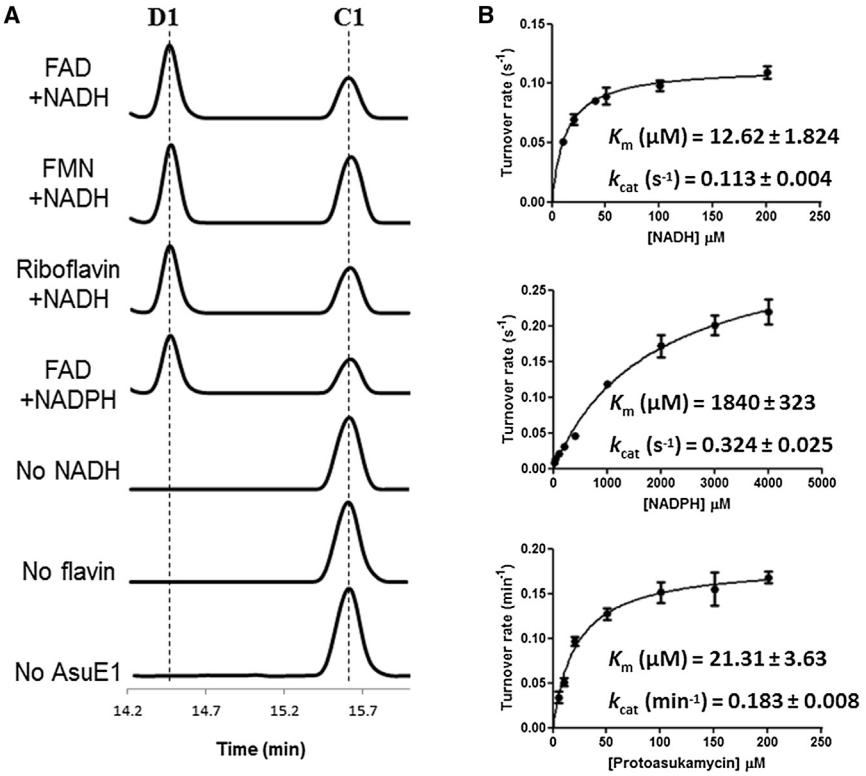

Figure 3. Characterization of AsuE1

(A) Extracted ion chromatograms showing the conversion of **C1** to **D1** catalyzed by AsuE1. The calculated mass with 10 ppm mass error tolerance was used.

(B) Determination of AsuE1 kinetic parameters. Error bars represent SDs from at least three independently performed experiments.

See also Figures S5 and S6.

AsuE1 with only a trace amount of flavin in vitro. These results suggested the importance of AsuE2 in vivo where the cellular concentration of free flavin is typically low, consistent with the observation that the Δ*asuE2* mutant accumulated the unmodified **C1** more than asukamycin (**A1**; Rui et al., 2010). AsuE1/E2 thus represents an atypical enzyme pair with a divergent evolutionary vestige and shows an indistinct boundary between the single- and two-component monooxygenases.

AsuE3 Is a Flavin-Dependent 4-Hydroxyprotoasukamycin Epoxidase

AsuE3 displays high sequence similarity (identity/similarity = 46%/63%) to LimB, which catalyzes the FAD- and NADH-dependent epoxidation of limonene to form limonene-1,2-epoxide in *Rhodococcus erythropolis* (van der Werf et al., 1999). The Δ*asuE3* mutant of *S. nodosus* accumulated **D1** (Rui et al., 2010), suggesting the identity of AsuE3 substrate. AsuE3 was purified from *E. coli* as a colorless protein without detectable amount of bound flavin. To determine the cofactor requirements and detailed reaction mechanism of AsuE3, the enzymatic reaction with **D1**, NADH, FMN, and AsuE3 was first examined. LC-MS analysis revealed the formation of a compound with a retention time and mass (m/z = 547.2437 $[M + H]^+$, ppm = 0.4) identical to that of the authentic **A1**. Omission of NADH, FMN, or AsuE3 led to a complete loss of activity. Substitution of FMN with FAD or riboflavin resulted in a more than 3-fold decrease of the reaction rate, indicating a stringency of AsuE3 toward flavin cofactors that differs from AsuE1 (Figure 5A). Similar to AsuE1 and E2, AsuE3 preferred NADH (k_{cat}/K_m = 4.3 $s^{-1}mM^{-1}$) over NADPH (k_{cat}/K_m = 0.24 $s^{-1}mM^{-1}$; Figure 5B). We next tested the possible effect of the flavin reductase AsuE2 to the activity of AsuE3. The addition of AsuE2 to the enzymatic reactions of AsuE3 under various conditions did not change the apparent reaction rates of asukamycin formation, different from a recent observation that a flavin reductase Fre stimulated the activity of epoxidase Lsd18 in polyether lasalocid biosynthesis (Minami et al., 2012). AsuE3 was therefore confirmed to be a single-component epoxidase catalyzing two half-reactions in the single protein: (1) reductive half-reaction using NADH and oxidized FMN to give reduced FMN, and (2) oxidative half-reaction using the reduced FMN and molecular oxygen to afford 4a-hydroperoxyflavin followed by epoxidation of the substrate. A similar epoxidation mechanism may be applied to the biosynthesis of a potent antibiotic methylenomycin A, because an AsuE3 homolog MmyO was identified in its putative biosynthetic gene cluster (Hornemann and Hopwood, 1978; Redenbach et al., 1998).

AsuE3 failed to oxidize **C1** in vitro, demonstrating that the protoasukamycin 4-hydroxylation catalyzed by AsuE1 was a prerequisite for epoxidation. Therefore, although both one-step and two-step monooxygenase mechanisms had been proposed for epoxyquinone formation (Hu and Floss, 2004; Thiericke et al., 1989), our biochemical characterization of AsuE1/E3 unequivocally supported the two-step mechanism for the formation of mC_7N in manumycin-type metabolites. The higher specific activity of AsuE3 toward **D1** (K_m = 7.20 μM, k_{cat} = 0.549 min^{-1}) compared to the activity of AsuE1 toward **C1** (K_m = 21.31 μM, k_{cat} = 0.183 min^{-1}) further suggesting that the first hydroxylation reaction promoted by AsuE1 was likely a rate-limiting step in the oxygenation cascade (Figures 5B and 6). AsuE3 also converted the 4-hydroxyprotoasukamycin derivatives (**D2**–**D5**) to the asukamycin derivatives (**A2**–**A5**; Figure S8), but had no activity toward compounds such as 4-isopropyl-6-methylcyclohex-2-enone, demonstrating a similar substrate tolerance of AsuE3 to AsuE1.

Alternative Starter Unit Feedings Based on Substrate Promiscuity of AsuA2

Based on the characterized substrate promiscuity of AsuA2, we performed precursor feeding experiments to generate manumycin-type products and to probe the flexibility of the overall biosynthetic pathway. This would also provide insights into the substrate specificity of AsuE1/E3 toward various substitutions

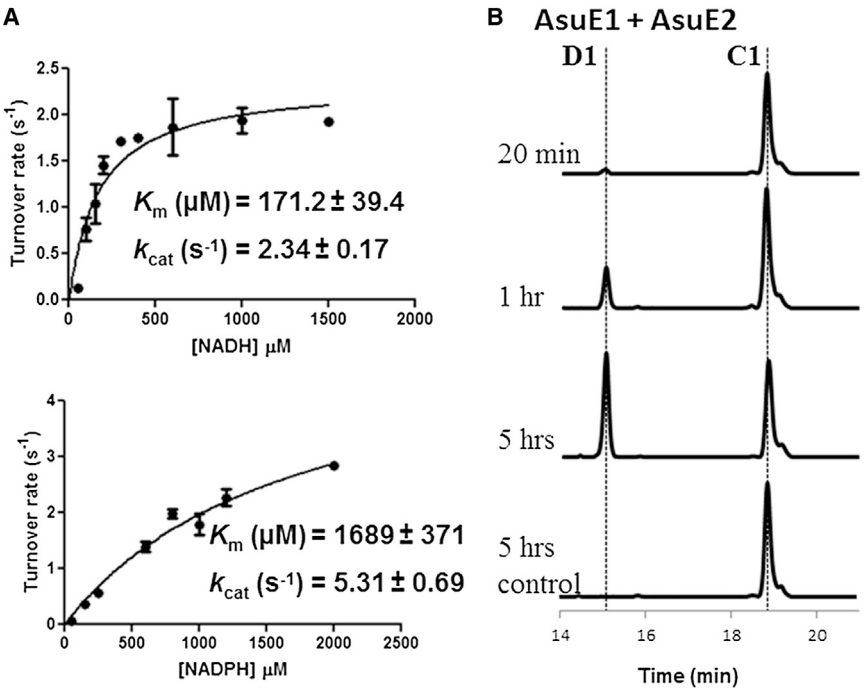

Figure 4. Characterization of AsuE2

(A) Determination of AsuE2 kinetic parameters. Error bars represent SDs from at least three independently performed experiments.

(B) Extracted ion chromatograms showing the conversion of **C1** to **D1** catalyzed by AsuE1/E2. The calculated mass with 10 ppm mass error tolerance was used. Assays contain 100 μM NADH, 100 μM protoasukamycin, 1 μM AsuE1, and 1 μM AsuE2. The control group lacks AsuE2 but contains 0.5 nM exogenous FMN.

See also Figure S7.

on the aromatic moiety in mC_7N formation. 3-ABA, 4-ABA, 4-HBA and 3,4-ACBA were supplemented to the overnight culture of Δ*asuA3* mutant (Rui et al., 2010) that did not produce asukamycins due to the deficiency in 3,4-AHBA formation. High-performance liquid chromatography (HPLC) and LC-MS revealed the successful incorporation of all compounds to the asukamycin biosynthetic machinery (Figures 7 and S9). Similar to a series of asukamycin-type compounds produced by wild-type, feeding of 3-ABA yielded a suite of major compounds containing the intact upper polyketide chains (**C6**–**C10**). 4-HBA lacks an amino group and was recruited to form **C13** without the attachment of upper polyketide chains. Likewise, 4-ABA was incorporated to form **C15** with an unmodified amino group as a minor product. The major product in the 4-ABA feeding experiment was **C16**, which was identified to be an *N*-acetylated **C15** by HRMS/MS analysis (Figure S9J). The acetyl group presumably resulted from the action of a nonspecific arylamine *N*-acetyltransferase, commonly found in cell to detoxify arylamine or arylhydroxylamine metabolites (Vineis et al., 1994). Notably, 3,4-ACBA was processed by the *asu* PKS to afford **C14** as the major product, which was fully characterized by MS and NMR analysis to be a halogenated asukamycin derivative containing a free amino group (Figures S9H and S10). The production of **C14** suggested that neither the amide synthetase AsuC2 encoded by the *asu* gene cluster nor a putative cellular arylamine *N*-acetyltransferase could modify the amino group of 3,4-ACB, possibly due to the steric hindrance of the chlorine atom. All of the asukamycin derivatives contained a non-oxygenated aromatic core structure, indicating the stringent substrate requirement of AsuE1 toward the regiospecific substitutions on the aromatic ring. It is notable that the catalytic functions of AsuE1/E3 were not affected by the structures of upper polyketide chain, since the Δ*asuC2* mutant with a deficiency for the upper chain attachment produced a significant amount of *N*-acetylated asukamycin derivative (**A8**) with an epoxyquinone moiety (Figure 1; Rui et al., 2010), and the replacement of the upper chain cyclohexyl group of asukamycin by different alicyclic and aliphatic moieties did not affect the formation of expoxyquinone (Hu and Floss, 2006; Pospíšil et al., 2011).

The manumycin family of natural products was previously demonstrated to have potent antibiotic activities against *Staphylococcus aureus* (Omura et al., 1976). Recently, methicillin-resistant *S. aureus* (MRSA) has emerged as a major pathogenic threat that is challenging to combat due to the resistance to nearly all available antibiotics (Fischbach and Walsh, 2009). To evaluate the antibiotic activity of asukamycins and their derivatives toward MRSA, agar diffusion assays were performed using *S. aureus* USA300 (SF8300), a wound-isolated MRSA strain that was implicated in numerous outbreaks (Diep et al., 2008). **A1** successfully inhibited the growth of MRSA, therefore establishing the potential of asukamycins for developing a new generation of anti-MRSA drugs. All generated metabolites (**C6**–**C16**) exhibited no activity toward MRSA, highlighting the importance of the epoxyquinone pharmacophore for antibiotic activities (Figure S11; Kohno et al., 1996; Sattler et al., 1998).

SIGNIFICANCE

We characterized the essential enzymes involved in the priming and postassembly modifications of 3,4-AHBA to yield the epoxyquinone pharmacophore in manumycin-type natural products. Our work demonstrated a two-step monooxygenase mechanism for the formation of epoxyquinone functionality, a warhead prevalent in natural products with a broad range of biologic activities. Based on the flexibility of asukamycin biosynthetic machinery, we further generated a group of manumycin-type metabolites through mutasynthesis and provided evidence for the critical role of the epoxyquinone moiety in the anti-MRSA activity of asukamycins.

EXPERIMENTAL PROCEDURES

Bacterial Strains, Culture Media, Plasmids, and Instrumentation

S. nodosus subsp. *asukaensis* ATCC 29757 was obtained from the American Type Culture Collection. *E. coli* BL21 Gold (DE3) and BL21 (DE3) plysS cells were purchased from Invitrogen. Bioassays with *S. aureus* USA300 (SF8300)

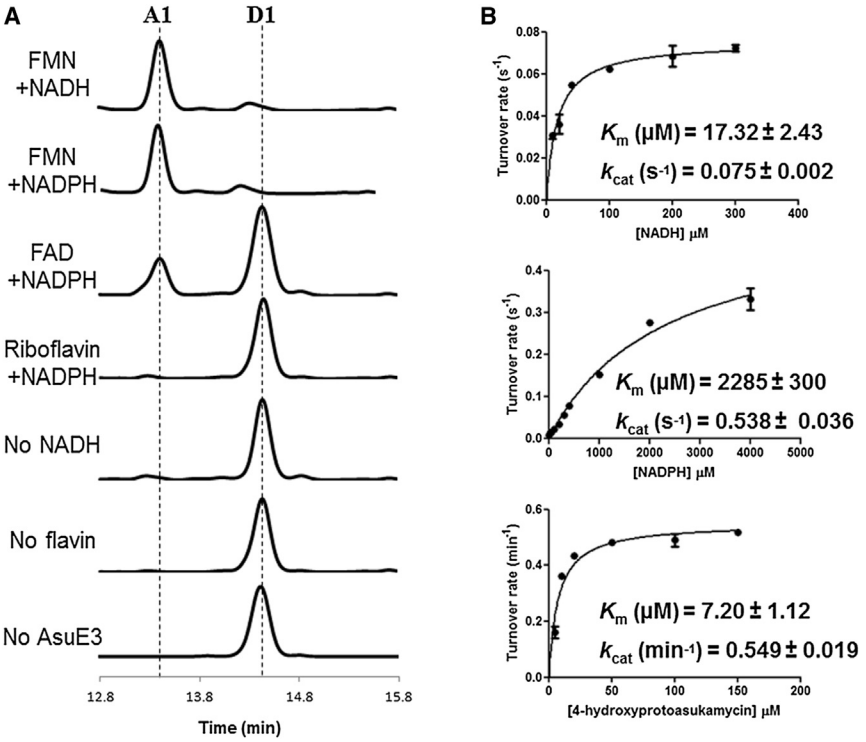

Figure 5. Characterization of AsuE3

(A) Extracted ion chromatograms showing the conversion of **D1** to **A1** catalyzed by AsuE3. The calculated mass with 10 ppm mass error tolerance was used.

(B) Determination of AsuE3 kinetic parameters. Error bars represent SDs from at least three independently performed experiments.

See also Figures S6 and S8.

were performed in Professor Binh Diep's lab in the Department of Medicine, San Francisco General Hospital. The media and chemicals were purchased from Difco, Sigma-Aldrich, and EMD Chemicals. Oligonucleotide primers were synthesized by Elim Biopharm, and PCR was performed with Phusion High-Fidelity PCR Master Mix (NEB). Cloning was performed using the Xa/LIC Cloning Kit (Novagen) or the restriction enzymes from NEB. Recombinant plasmid DNA was purified with a QIAprep kit (QIAGEN). DNA sequencing was performed at the UC Berkeley DNA Sequencing Facility. SDS-PAGE gels and nickel-nitrilotriacetic acid agarose (Ni-NTA) superflow resin were purchased from Biorad and QIAGEN, respectively. Protein samples were concentrated using the 10 kDa or 30 kDa cutoff Amicon Ultra-15 Centrifugal Filter Units (Millipore). DNA and protein concentrations were determined by Nanodrop 1000 spectrophotometer (Thermo Scientific). HPLC analysis was performed on an Agilent 1260 Infinity system with Inertsil ODS-4 C18 column (5 μm, 4.6 × 250 mm). LC-MS analysis was carried out on an Agilent Technologies 6520 Accurate-Mass Q-TOF LC-MS instrument equipped with an Agilent Eclipse Plus C18 column (3.5 μm, 4.6 × 100 mm). ^{1}H-nuclear magnetic resonance (NMR), ^{13}C-NMR, heteronuclear single quantum correlation, and heteronuclear multiple bond correlation spectra were recorded in d_6-DMSO on a Bruker Biospin 900 MHz spectrometer with a cryoprobe.

Cloning, Overexpression, and Purification of AsuA2, AsuC11, AsuC12, and AsuE1-E3

The corresponding proteins (AsuA2, 51 kDa; AsuC11 and AsuC12, 10 kDa; AsuE1, 43 kDa; AsuE2, 19 kDa; AsuE3, 41 kDa) were overproduced in *E. coli* cells and purified using Ni-NTA affinity chromatography (Figure S2). First, *asuA2*, *asuC11*, *asuC12*, and *asuE1-E3* were PCR-amplified from cosmid pART1361 with the primers shown in Table S1. For AsuA2, gel-purified PCR products were ligated to pET-30 Xa/LIC to yield pZR01 following the standard protocol. For AsuC11 and AsuC12, PCR products were digested with NdeI/EcoRI and inserted into the NdeI/EcoRI cut pET-24b to give pZR02 and pZR03, respectively. For AsuE1-E3, PCR products were digested with BglII/HindIII and inserted into BamHI/HindIII cut pRSETB to afford pART1321/1301/1311, respectively. All plasmid constructs were confirmed by DNA sequencing. Then, pZR01 was expressed in *E. coli* BL21 Gold (DE3); pZR02 and pZR03 were expressed in *E. coli* BAP1; pART1321/1301/1311 were expressed in *E. coli* BL21 (DE3) plysS. *E. coli* BAP1 strain that contains a chromosomal copy of the phosphopantetheinyl transferase Sfp was used for AsuC11 and C12 expression to ensure their posttranslational modification to the pantetheinylated forms (Pfeifer et al., 2001). For expressions of AsuA2, AsuC11, and AsuC12, the cells were grown at 37°C in 1 l of LB medium supplemented with 50 μg/ml kanamycin, and then induced at 16°C and optical density 600 of 0.4–0.6 with 0.1 mM of isopropyl-β-D-thiogalactopyranoside (IPTG) for 16 hr. For expression of AsuE1-E3, the cells were grown in 1 l of LB medium containing 2.5 mM betaine and 1 M sorbitol with 100 μg/ml of ampicillin and 25 μg/ml of chloramphenicol, induced, and harvested as described above. The cells were resuspended in 35 ml of lysis buffer (20 mM HEPES, pH 7.5, 0.5 M NaCl, and 5 mM imidazole), and lysed by sonication on ice. The soluble proteins were collected by centrifugation at 12,000 × *g* and 4°C for 1 hr, and mixed with 1 ml of Ni-NTA agarose resin on a nutator at 4°C for 1 hr. The proteins were then loaded onto a gravity flow column, washed with washing buffer (20 mM HEPES, pH 7.5, and 20 mM imidazole), and eluted with eluting buffer (20 mM HEPES, pH 7.5, and 150 mM imidazole). Purified proteins were concentrated into 20 mM of HEPES (pH 7.5) with 10% glycerol using Amicon Centrifugal Filter Units, flash-frozen in liquid nitrogen, and stored at −80°C. The approximate protein yields were 0.9 mg/l for AsuA2, 17 mg/l for AsuC11, 6.7 mg/l for AsuC12, 1.5 mg/l for AsuE1, 1.8 mg/l for AsuE2, and 1.8 mg/l for AsuE3.

ATP-[^{32}P]PP$_i$ Exchange Assay

The assays were performed in 100 μl of reaction mixture that contains 50 mM Tris buffer (pH 7.5), 2 mM $MgCl_2$, 5 mM ATP, 1 mM Na_4PP_i (containing 250–400 kcpm of Na_4[^{32}P]PP_i), 1 mM TCEP, 5 mM aromatic substrate, and 1 μM AsuA2 at 25°C. Reactions were initiated by adding AsuA2 and quenched with 500 μl of a charcoal suspension (100 mM Na_4PP_i, 350 mM $HClO_4$, and 16 g/l charcoal) after 60 min. The pellets were collected by centrifugation and washed twice with 500 μl of washing solution (100 mM Na_4PP_i and 350 mM $HClO_4$). AsuA2 kinetic analysis was carried out in 500 μl of reaction mixture as described above except for a varying concentration of 3,4-AHBA (5, 10, 20, 50, 100, or 250 μM). Reactions were initiated by adding AsuA2 and quenched with 500 μl of a charcoal suspension at 0, 5, 10, 15, and 20 min. The rate of substrate consumption was calculated as the incorporation rate of the charcoal-bound [^{32}P]-ATP measured on a Beckman LS 6500 scintillation counter. The resulting data were fitted to the Michaelis-Menten equation in GraphPad Prism to obtain estimates for k_{cat} and K_m.

LC-MS Identification of ACP-Bound Biosynthetic Intermediate

Assays were performed in 50 μl of 50 mM Tris (pH 7.5), 2 mM $MgCl_2$, 1 mM TCEP, 5 mM ATP, 1 mM aromatic substrate, 1 μM AsuA2, and 1 μM AsuC12 or AsuC11. Reactions were incubated for 1 hr and analyzed with nanocapillary LC-MS using a chip column (Agilent Zorbax 300SB-C18 5 μm; separation: 43 mm × 75 μm; enrichment: 4 mm 40 nl) in line with a QTOF (Agilent 6510 Q-TOF LC-MS). A linear gradient of 2%–95% CH_3CN over 9 min in H_2O with 0.1% formic acid at a flow rate of 0.6 μl/min was used for analysis. The protein mass was determined by deconvolution using MassHunter Qualitative Analysis (Agilent).

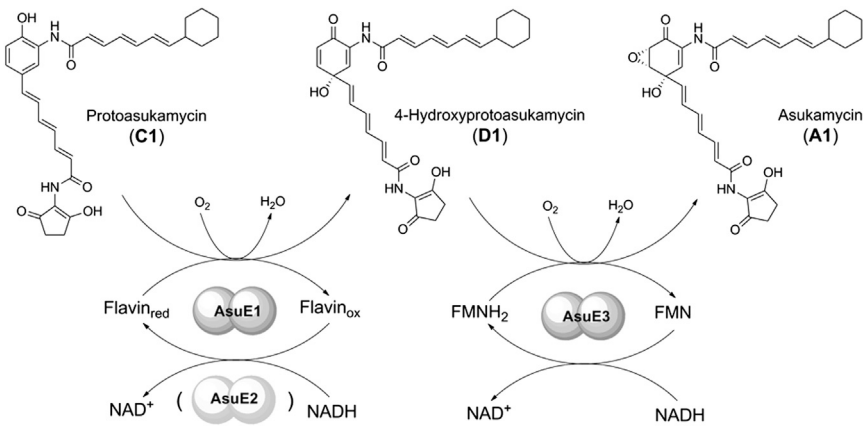

Figure 6. Schematic of the Epoxyquinone Moiety Formation in Asukamycin
See also Figure S2 and Table S1.

AsuE1 and AsuE3 Enzymatic Assays

The authentic protoasukamycin and 4-hydroxyprotoasukamycin were obtained from the fermentation cultures of Δ*asuE1* and Δ*asuE3* mutants, respectively, as described previously (Rui et al., 2010). Typical conditions were: a 50 μl AsuE1 or AsuE3 reaction mixture contains 50 mM phosphate buffer (pH 7.0), 1 mM NAD(P)H, 20 μM flavin, 200 μM of either protoasukamycin or 4-hydroxyprotoasukamycin, and 10 μM of either AsuE1 or AsuE3, respectively. The reaction was performed at 30°C and quenched with an equal volume of ethyl acetate. The organic layer was concentrated in vacuo and resuspended into 50 μl of methanol. Two microliters of the solution was injected into LC-MS and a linear gradient of 55%–95% CH_3CN (vol/vol) over 15 min in H_2O with 0.1% (vol/vol) formic acid at a flow rate of 0.5 ml/min was used for analysis.

To obtain the kinetic parameters for NADH/NADPH, 100 μl of AsuE1 or AsuE3 assays were performed in 50 mM phosphate buffer (pH 7.0), 20 μM flavin (FAD for AsuE1 and FMN for AsuE3), 1 μM either AsuE1 or AsuE3, and variable concentrations of NADH/NADPH. The decrease in absorbance at 340 nm was monitored after the addition of enzyme in a Greiner UV-Star 96-well plate on a Tecan Infinite 200 Pro plate reader. The acquired turnover rates were fit to the Michaelis-Menten equation using GraphPad Prism to obtain k_{cat} and K_m.

To obtain the kinetic parameters of AsuE1 for protoasukamycin, 1 ml of AsuE1 assay was performed in 50 mM phosphate buffer (pH 7.0), 20 μM FAD, 1 mM NADH, 1 μM AsuE1, and variable concentrations of protoasukamycin. Aliquots of 200 μl were quenched at 3, 5, 7, 9, and 11 min using an equal volume of ethyl acetate. The extraction method and LC-MS analysis were the same as mentioned before. The quantification of 4-hydroxyprotoasukamycin was conducted by integrating the extracted 4-hydroxyprotoasukamycin peak. The acquired turnover rates were fit to the Michaelis-Menten equation using GraphPad Prism to obtain k_{cat} and K_m. The determination of kinetic parameters of AsuE3 for 4-hydroxyprotoasukamycin was similar to that of AsuE1, except that FMN was used as the flavin cofactor and the production of asukamycin was recorded for calculation.

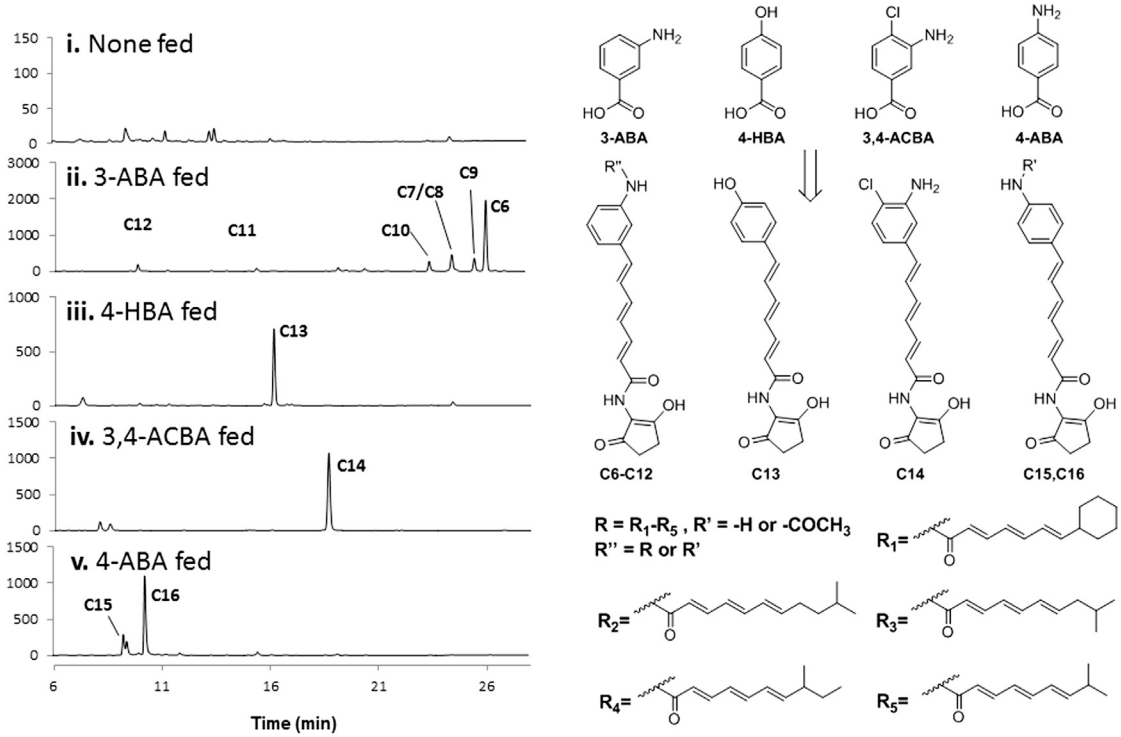

Figure 7. HPLC Analysis of Asukamycin Derivatives in Δ*asuA3* Supplemented with 3-ABA, 4-ABA, 4-HBA, and 3,4-ACBA
R′ = -H in **C12** and **C15**; R′ = -$COCH_3$ in **C11** and **C16**; R = R_1–R_5 in **C6–C10**; λ = 325 nm.
Δ*asuA3*, 3,4-AHBA deficient mutant.
See also Figures S9–S11.

LC-MS Analysis of Flavin Bound to AsuE2

Ten nanomoles of AsuE2 was denatured by addition of methanol to release any bound cofactor. After centrifugation, the supernatant was analyzed with LC-MS using a linear gradient from 5% to 95% acetonitrile containing 0.1% formic acid at a flow rate of 0.5 ml/min. The released flavin was detected in the negative ion mode; 200 pmol of authentic FAD and FMN were used as standard.

AsuE2 Activity Analysis

One hundred microliters of reaction mixture contains 50 mM phosphate buffer (pH 7.0), 1 μM AsuE2, 10 μM of FMN, and variable amounts of NAD(P)H at 30°C. The decrease in absorbance at 340 nm was monitored after the addition of enzyme in a 96-well plate on a plate reader. Steady-state kinetic constants for NAD(P)H were performed using a fixed FMN concentration at 10 μM and variable NAD(P)H concentrations at a 90 s interval. The acquired turnover rates were fit to the Michaelis-Menten equation using GraphPad Prism to obtain k_{cat} and K_m.

Small-Scale Production of Asukamycin Derivatives by Mutasynthesis

A single colony of *S. nodosus* Δ*asuA3* mutant was cultured in 25 ml of YMG media (4 g/l yeast extract, 10 g/l malt extract, and 4 g/l glucose) in a baffled flask with the coil at 30°C with constant shaking (250 rpm). One millimolar 3,4-AHBA or the aromatic derivatives were added to 1-day-old cultures and continued to culture for 2 more days. Fermented cultures were mixed thoroughly with an equal volume of ethyl acetate. The mixture was separated by centrifugation, and the ethyl acetate layer was collected and evaporated to near dryness. The crude extract was dissolved in an equal volume of methanol and analyzed using HPLC at a flow rate of 1 ml/min at 25°C. One hundred microliters of crude extract was injected, equilibrated with 30% CH_3CN in H_2O with 0.1% formic acid for 3 min, developed with a gradient of 30%–95% CH_3CN in H_2O with 0.1% formic acid for 20 min, and washed with 90% CH_3CN in H_2O with 0.1% formic acid for 10 min. LC-MS was carried out using the same elution program. A collision energy of 10 V was used for all tandem mass spectroscopy experiments.

Large-Scale Production, Purification, and Characterization of C14

To purify milligrams of compound **C14**, 40 flasks of 25 ml of cultures were grown and supplemented with 1 mM 3-amino-4-chlorobenzoic acid (3,4-ACBA). The harvested cultures were combined and extracted three times with an equal volume of ethyl acetate. The ethyl acetate layer was dried, concentrated, and purified through a Sep-Pak C18 cartridge to give 10 mg **C14** for NMR analysis.

Bioactivity Analysis

Antibiotic activity of asukamycin and derivatives was examined with an agar diffusion assay. *S. aureus* USA300 (SF8300) was cultured in TSB medium at 37°C overnight, and 25 μl of this seed culture was diluted in 400 μl of TSB and streaked out on the blood agar plate (BD). Ten microgram test compounds were dissolved in 20 μl of ethyl acetate or methanol, loaded on a sterile filter paper disk (7 mm diameter), air-dried, and placed on the plates, which were incubated at 37°C for 24 hr.

SUPPLEMENTAL INFORMATION

Supplemental Information includes eleven figures and one table and can be found with this article online at http://dx.doi.org/10.1016/j.chembiol.2013.05.006.

ACKNOWLEDGMENTS

We are grateful to B. Diep and H. Le (San Francisco General Hospital) for MRSA bioassay experiments. We thank R. Sarpong (UC Berkeley) for providing various benzoic acids, J. Pelton (UC Berkeley) for helping with NMR spectroscopic analysis, and S. Bauer (UC Berkeley) for helping with MS analysis. This work was supported by Berkeley and EBI startup funds, a Faculty Research Grant, and the Pew Scholars Program.

Received: February 20, 2013
Revised: April 23, 2013
Accepted: May 9, 2013
Published: July 25, 2013

REFERENCES

Ballou, D.P., Entsch, B., and Cole, L.J. (2005). Dynamics involved in catalysis by single-component and two-component flavin-dependent aromatic hydroxylases. Biochem. Biophys. Res. Commun. *338*, 590–598.

Bernier, M., Kwon, Y.K., Pandey, S.K., Zhu, T.N., Zhao, R.J., Maciuk, A., He, H.J., Decabo, R., and Kole, S. (2006). Binding of manumycin A inhibits IkappaB kinase beta activity. J. Biol. Chem. *281*, 2551–2561.

Cole, L.J., Gatti, D.L., Entsch, B., and Ballou, D.P. (2005). Removal of a methyl group causes global changes in *p*-hydroxybenzoate hydroxylase. Biochemistry *44*, 8047–8058.

Diep, B.A., Palazzolo-Ballance, A.M., Tattevin, P., Basuino, L., Braughton, K.R., Whitney, A.R., Chen, L., Kreiswirth, B.N., Otto, M., DeLeo, F.R., and Chambers, H.F. (2008). Contribution of Panton-Valentine leukocidin in community-associated methicillin-resistant *Staphylococcus aureus* pathogenesis. PLoS ONE *3*, e3198.

Entsch, B., Cole, L.J., and Ballou, D.P. (2005). Protein dynamics and electrostatics in the function of *p*-hydroxybenzoate hydroxylase. Arch. Biochem. Biophys. *433*, 297–311.

Ferreras, J.A., Stirrett, K.L., Lu, X.Q., Ryu, J.S., Soll, C.E., Tan, D.S., and Quadri, L.E.N. (2008). Mycobacterial phenolic glycolipid virulence factor biosynthesis: mechanism and small-molecule inhibition of polyketide chain initiation. Chem. Biol. *15*, 51–61.

Fischbach, M.A., and Walsh, C.T. (2009). Antibiotics for emerging pathogens. Science *325*, 1089–1093.

Hara, M., Akasaka, K., Akinaga, S., Okabe, M., Nakano, H., Gomez, R., Wood, D., Uh, M., and Tamanoi, F. (1993). Identification of Ras farnesyltransferase inhibitors by microbial screening. Proc. Natl. Acad. Sci. USA *90*, 2281–2285.

Herath, K.B., Jayasuriya, H., Bills, G.F., Polishook, J.D., Dombrowski, A.W., Guan, Z., Felock, P.J., Hazuda, D.J., and Singh, S.B. (2004). Isolation, structure, absolute stereochemistry, and HIV-1 integrase inhibitory activity of integrasone, a novel fungal polyketide. J. Nat. Prod. *67*, 872–874.

Hornemann, U., and Hopwood, D.A. (1978). Isolation and characterization of desepoxy-4,5-didehydro-methylenomycin-A, precursor of antibiotic methylenomycin-A in Scp1+ strains of *Streptomyces Coelicolor* A3(2). Tetrahedron Lett. *33*, 2977–2978.

Hu, Y.D., and Floss, H.G. (2004). Further studies on the biosynthesis of the manumycin-type antibiotic, asukamycin, and the chemical synthesis of protoasukamycin. J. Am. Chem. Soc. *126*, 3837–3844.

Hu, Y.D., and Floss, H.G. (2006). Starter unit specificity of the asukamycin "upper" chain polyketide synthase and the branched-chain fatty acid synthase of *Streptomyces nodosus* subsp *asukaensis*. Heterocycles *69*, 133–149.

Hu, Y.D., Melville, C.R., Gould, S.J., and Floss, H.G. (1997). 3-amino-4-hydroxybenzoic acid: The precursor of the C_7N unit in asukamycin and manumycin. J. Am. Chem. Soc. *119*, 4301–4302.

Kamiyama, H., Usui, T., Uramoto, M., Takagi, H., Shoji, M., Hayashi, Y., Kakeya, H., and Osada, H. (2008). Fungal metabolite, epoxyquinol B, cross-links proteins by epoxy-thiol conjugation. J. Antibiot. *61*, 94–97.

Kim, S.H., Hisano, T., Iwasaki, W., Ebihara, A., and Miki, K. (2008). Crystal structure of the flavin reductase component (HpaC) of 4-hydroxyphenylacetate 3-monooxygenase from *Thermus thermophilus* HB8: Structural basis for the flavin affinity. Proteins *70*, 718–730.

Kohno, J., Nishio, M., Kawano, K., Nakanishi, N., Suzuki, S., Uchida, T., and Komatsubara, S. (1996). TMC-1 A, B, C and D, new antibiotics of the manumycin group produced by Streptomyces sp. Taxonomy, production, isolation, physico-chemical properties, structure elucidation and biological properties. J. Antibiot. *49*, 1212–1220.

Koizumi, F., Ishiguro, H., Ando, K., Kondo, H., Yoshida, M., Matsuda, Y., and Nakanishi, S. (2003). EI-1941-1 and -2, novel interleukin-1 beta converting enzyme inhibitors Produced by Farrowia sp. E-1941. II. Taxonomy of

producing strain, fermentation, isolation, physico-chemical properties, and biological properties. J. Antibiot. *56*, 603–609.

Minami, A., Shimaya, M., Suzuki, G., Migita, A., Shinde, S.S., Sato, K., Watanabe, K., Tamura, T., Oguri, H., and Oikawa, H. (2012). Sequential enzymatic epoxidation involved in polyether lasalocid biosynthesis. J. Am. Chem. Soc. *134*, 7246–7249.

Miyashita, K., and Imanishi, T. (2005). Syntheses of natural products having an epoxyquinone structure. Chem. Rev. *105*, 4515–4536.

Nakashima, T., Tanaka, R., Yamashita, Y., Kanda, Y., and Hara, M. (2008). Aranorosin and a novel derivative inhibit the anti-apoptotic functions regulated by Bcl-2. Biochem. Biophys. Res. Commun. *377*, 1085–1090.

Omura, S., Kitao, C., Tanaka, H., Oiwa, R., Takahashi, Y., Nakagawa, A., Shimada, M., and Iwai, Y. (1976). A new antibiotic, asukamycin, produced by Streptomyces. J. Antibiot. *29*, 876–881.

Pfeifer, B.A., Admiraal, S.J., Gramajo, H., Cane, D.E., and Khosla, C. (2001). Biosynthesis of complex polyketides in a metabolically engineered strain of E. coli. Science *291*, 1790–1792.

Pfennig, F., Schauwecker, F., and Keller, U. (1999). Molecular characterization of the genes of actinomycin synthetase I and of a 4-methyl-3-hydroxyanthranilic acid carrier protein involved in the assembly of the acylpeptide chain of actinomycin in *Streptomyces*. J. Biol. Chem. *274*, 12508–12516.

Pospíšil, S., Petříčková, K., Sedmera, P., Halada, P., Olšovská, J., and Petříček, M. (2011). Effect of starter unit availability on the spectrum of manumycin-type metabolites produced by *Streptomyces nodosus* ssp. *asukaensis*. J. Appl. Microbiol. *111*, 1116–1128.

Redenbach, M., Ikeda, K., Yamasaki, M., and Kinashi, H. (1998). Cloning and physical mapping of the EcoRI fragments of the giant linear plasmid SCP1. J. Bacteriol. *180*, 2796–2799.

Rui, Z., Petrícková, K., Skanta, F., Pospísil, S., Yang, Y.L., Chen, C.Y., Tsai, S.F., Floss, H.G., Petrícek, M., and Yu, T.W. (2010). Biochemical and genetic insights into asukamycin biosynthesis. J. Biol. Chem. *285*, 24915–24924.

Sandy, M., Rui, Z., Gallagher, J., and Zhang, W. (2012). Enzymatic synthesis of dilactone scaffold of antimycins. ACS Chem. Biol. *7*, 1956–1961.

Sattler, I., Thiericke, R., and Zeeck, A. (1998). The manumycin-group metabolites. Nat. Prod. Rep. *15*, 221–240.

Sekizawa, R., Ikeno, S., Nakamura, H., Naganawa, H., Matsui, S., Iinuma, H., and Takeuchi, T. (2002). Panepophenanthrin, from a mushroom strain, a novel inhibitor of the ubiquitin-activating enzyme. J. Nat. Prod. *65*, 1491–1493.

Singh, S.B., Zink, D.L., Liesch, J.M., Ball, R.G., Goetz, M.A., Bolessa, E.A., Giacobbe, R.A., Silverman, K.C., Bills, G.F., Pelaez, F., et al. (1994). Preussomerins and deoxypreussomerins - novel inhibitors of Ras farnesyl-protein transferase. J. Org. Chem. *59*, 6296–6302.

Sugita, M., Sugita, H., and Kaneki, M. (2007). Farnesyltransferase inhibitor, manumycin a, prevents atherosclerosis development and reduces oxidative stress in apolipoprotein E-deficient mice. Arterioscler. Thromb. Vasc. Biol. *27*, 1390–1395.

Suzuki, H., Ohnishi, Y., Furusho, Y., Sakuda, S., and Horinouchi, S. (2006). Novel benzene ring biosynthesis from C(3) and C(4) primary metabolites by two enzymes. J. Biol. Chem. *281*, 36944–36951.

Tanaka, T., Tsukuda, E., Uosaki, Y., and Matsuda, Y. (1996). EI-1511-3, -5 and EI-1625-2, novel interleukin-1 beta converting enzyme inhibitors produced by Streptomyces sp. E-1511 and E-1625. III. Biochemical properties of EI-1511-3, -5 and EI-1625-2. J. Antibiot. *49*, 1085–1090.

Thiericke, R., Zeeck, A., Robinson, J.A., Beale, J.M., and Floss, H.G. (1989). The biosynthesis of manumycin - origin of the oxygen and nitrogen-atoms. J. Chem. Soc. Chem. Comm. 402–403.

van Berkel, W.J.H., Kamerbeek, N.M., and Fraaije, M.W. (2006). Flavoprotein monooxygenases, a diverse class of oxidative biocatalysts. J. Biotechnol. *124*, 670–689.

van der Werf, M.J., Swarts, H.J., and de Bont, J.A.M. (1999). *Rhodococcus erythropolis* DCL14 contains a novel degradation pathway for limonene. Appl. Environ. Microbiol. *65*, 2092–2102.

Vineis, P., Bartsch, H., Caporaso, N., Harrington, A.M., Kadlubar, F.F., Landi, M.T., Malaveille, C., Shields, P.G., Skipper, P., Talaska, G., et al. (1994). Genetically based *N*-acetyltransferase metabolic polymorphism and low-level environmental exposure to carcinogens. Nature *369*, 154–156.

Webb, B.N., Ballinger, J.W., Kim, E., Belchik, S.M., Lam, K.S., Youn, B., Nissen, M.S., Xun, L.Y., and Kang, C. (2010). Characterization of chlorophenol 4-monooxygenase (TftD) and NADH:FAD oxidoreductase (TftC) of *Burkholderia cepacia* AC1100. J. Biol. Chem. *285*, 2014–2027.

Zheng, Z.H., Dong, Y.S., Zhang, H., Lu, X.H., Ren, X., Zhao, G.Y., He, J.G., and Si, S.Y. (2007). Isolation and characterization of N98-1272 A, B and C, selective acetylcholinesterase inhibitors from metabolites of an actinomycete strain. J. Enzyme Inhib. Med. Chem. *22*, 43–49.